[13] A. Taflove, *Computational Electrodynamics: The Finite-Difference Time-Domain Method*. Norwood, MA: Artech House, 1995, pp. 76–77.

[14] X. P. Liang and K. A. Zaki, "Modeling of cylindrical dielectric resonators in rectangular waveguides and cavities," *IEEE Trans. Microwave Theory Tech.*, vol. 41, pp. 2174–2181, Dec. 1993.

[15] D. Kajfez, A. W. Guillon, and J. James, "Computed modal-field distributions for isolated dielectric resonators," *IEEE Trans. Microwave Theory Tech.*, vol. MTT-32, pp. 1609–1616, Dec. 1984.

A Pole-Free Modal Field-Matching Technique for Eigenvalue Problems in Electromagnetics

Smain Amari and Jens Bornemann

***Abstract*— A pole-free formulation of the modal field-matching technique (MFMT) as applied to eigenvalue problems in electromagnetics is presented in this paper. The poles in the determinantal equation are systematically *eliminated*, without requiring previous knowledge of their locations or nature, resulting in well-behaved determinants. The minimum singular value in a singular-value decomposition of the pole-free matrix exhibits much wider dips than what is obtained from the standard MFMT. The pole-free formulation is applied to determine the cutoff wavenumbers of a ridged waveguide to demonstrate its validity and efficiency.**

***Index Terms*— Eigenvalues/eigenfunctions, mode-matching methods, ridge waveguides.**

I. Introduction

A large number of problems in engineering, physics, and applied mathematics are reduced to solving a homogeneous matrix equation of the form

$$[A(k)][x] = 0 \tag{1}$$

where $[A(k)]$ is a parameter-dependent square complex matrix of order $n \times n$ and x is an unknown n-element column vector [1], [2]. Nontrivial solutions to (1) exist only when the matrix $[A]$ is singular, i.e., when its determinant vanishes for certain values of the parameter k:

$$\det[A(k)] = 0, \qquad k = k_0. \tag{2}$$

The numerical solution of (2) is often hindered by the presence of poles in the determinant in the vicinity of its zeros, thereby leading to a time-consuming search and nonphysical roots. This situation is often encountered in the application of the modal field-matching technique (MFMT) to determining cutoff frequencies and propagation constants of microwave and millimeter-wave structures.

A few attempts have been made to eliminate poles from specific applications in the recent years. In [3], a pole–zero combination was used in the determination of spectrum of unilateral finline. In [4], a pole-free function was constructed once the locations of the poles were determined. In both approaches, the accurate determination of the pole locations is required in a first step in order to reliably detect the zeros in the second step.

Manuscript received October 29, 1996; revised March 7, 1997.

The authors are with the Laboratory for Lightwave Electronics, Microwaves and Communications, LLiMiC, Department of Electrical and Computer Engineering, University of Victoria, Victoria, B.C., Canada V8W 3P6.

Publisher Item Identifier S 0018-9480(97)06073-0.

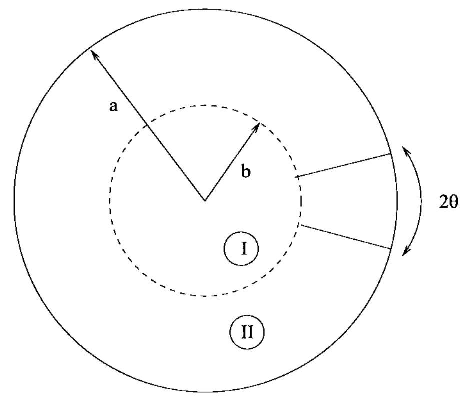

Fig. 1. Cross section of a ridged circular waveguide.

A direct way in avoiding the poles consists of maintaining the original equations as obtained from the boundary conditions. The large size of the resulting matrix requires large central processing unit (CPU) times especially when large numbers of modes are needed. When equal numbers of modes are retained in the modal expansions, it is possible to eliminate the poles from the determinantal equation. However, the resulting determinant is practically a rectangular function, thereby adding to the CPU times required to accurately locate its zeros [5].

A technique to circumvent these poles was presented by Labay and Bornemann where the singular-value decomposition of the matrix $[A(k)]$ is used instead of its determinant [6]. In this approach, nontrivial solutions to (1) are determined from the zeros of the smallest singular value in the singular-value decomposition of the matrix $[A(k)]$ [6].

It is important to note that this approach, despite its success in reformulating the problem through a pole-free quantity, does not eliminate the poles from the matrix $[A(k)]$. In fact, the poles in the determinant are reflected in the singular-value approach through the sharpness of the minima. The sharpness of a minimum in the smallest singular value increases as its location approaches a pole of the determinant. This will be shown by the numerical results of this paper.

Here we reexamine the origin of the poles in the determinant within the MFMT and show how they can be systematically eliminated from the matrix $[A(k)]$ without requiring prior knowledge of their locations. These poles result from the inversion of singular matrices in the construction of the matrix $[A(k)]$. By carefully avoiding such operations, we show how well-behaved determinants can be obtained. The resulting determinant is inherently pole-free and the minima of the smallest singular value are broader than in the standard MFMT.

II. A Pole-Free Modal Field-Matching Technique

We focus attention on the structure shown in Fig. 1. The ridge of thickness 2θ and depth $h = a - b$ and the metallic walls of the waveguide are assumed lossless. Here, we present only the analysis of the transverse-electric (TE) modes as these are sufficient to illustrate the approach.

The TE modes can be divided into two sets with either an electric or a magnetic wall along its plane of symmetry. The case of the electric-wall symmetry is treated in details, although numerical results for the cutoff wavenumbers will be given for both symmetries.

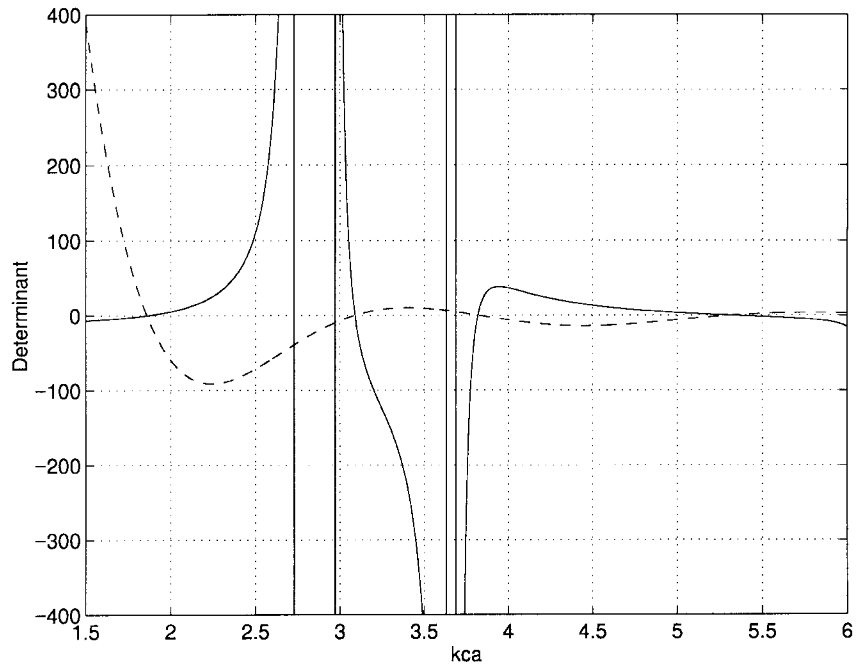

Fig. 2. Determinant of $[A(k_c)]$ as a function of k_ca when $h/a = 0.5, \theta = 2.29°$, and $M = N = 3$ from the standard MFMT (solid line) and the pole-free MFMT (dashed line).

Following the analysis presented in [7], we expand the axial magnetic field in each of the two regions. From the boundary conditions at the interface I–II, we get two sets of homogeneous equations in the expansion coefficients in the two regions

$$
\begin{aligned}
[A] &= [C][B] \\
[B] &= [D][A].
\end{aligned} \tag{3}
$$

The square matrices $[C]$ and $[D]$ are given by

$$
[C]_{nm} = \frac{J_l'(k_cb)Y_l'(k_ca) - Y_l'(k_cb)J_l'(k_ca)}{J_{n-1}'(k_cb)} \times \int_\theta^{2\pi-\theta} d\phi \frac{\cos[(n-1)\phi]}{\sqrt{\pi(1+\delta_{n1})}} \cdot \frac{\cos[(m-1)\pi\dfrac{\phi-\theta}{\pi-\theta}]}{\sqrt{(\pi-\theta)(1+\delta_{m1})}} \tag{4a}
$$

and

$$
[D]_{mn} = \frac{J_{n-1}(k_cb)}{J_l(k_cb)Y_l'(k_ca) - Y_l(k_cb)J_l'(k_ca)} \times \int_\theta^{2\pi-\theta} d\phi \frac{\cos[(n-1)\phi]}{\sqrt{\pi(1+\delta_{n1})}} \cdot \frac{\cos[(m-1)\pi\dfrac{\phi-\theta}{\pi-\theta}]}{\sqrt{(\pi-\theta)(1+\delta_{m1})}}. \tag{4b}
$$

Here, $l = m\pi/(\pi - \theta)$ and J_l and Y_l are Bessel and Neumann functions of order l, respectively. Equation (3) can be used to eliminate one set of coefficients leading to the following determinantal equation:

$$
\det\{[D][C] - [U]\} = 0. \tag{5}
$$

Here, $[U]$ is the $N \times N$ unit matrix. The cutoff wavenumbers are given by the roots of (5).

The solid line in Fig. 2 is a plot of the determinant in (5) as a function of k_ca when $b/a = 0.5$ and $N = 3$. The presence of the poles is evident. Most importantly, the determinant changes sign in the vicinity of a pole, thereby leading to nonphysical solutions.

In order to remove the poles from the formulation, we first have to identify the terms causing the singularities. From (4), it is evident that only the divisions by the terms $J_{n-1}'(k_cb)$ and $J_l(k_cb)Y_l'(k_ca) - Y_l(k_cb)J_l'(k_ca)$ can cause the singularities in the determinant as the coupling integrals are finite. In addition, the Bessel functions in the numerators in (4) are evaluated away from the origin as $k_c = 0$ is not a possible solution, and are consequently all finite. We, therefore, proceed to eliminate these divisions from the final determinantal equation giving the cutoff wavenumbers.

We start from the boundary conditions of E_ϕ which lead to

$$
J_{n-1}'(k_cb)A_n = \sum_{m=1}^{M} B_m[J_l'(k_cb)Y_l'(k_ca) - Y_l'(k_cb)J_l'(k_ca)] \times \int_\theta^{2\pi-\theta} d\phi \frac{\cos[(n-1)\phi]}{\sqrt{\pi(1+\delta_{n1})}} \cdot \frac{\cos[(m-1)\pi\dfrac{\phi-\theta}{\pi-\theta}]}{\sqrt{(\pi-\theta)(1+\delta_{m1})}}. \tag{6a}
$$

The continuity of the magnetic field leads to a similar equation:

$$
[J_l(k_cb)Y_l'(k_ca) - Y_l(k_cb)J_l'(k_ca)]B_m = \sum_{n=1}^{M} J_{n-1}(k_cb)A_n \times \int_\theta^{2\pi-\theta} d\phi \frac{\cos[(n-1)\phi]}{\sqrt{\pi(1+\delta_{n1})}} \cdot \frac{\cos[(m-1)\pi\dfrac{\phi-\theta}{\pi-\theta}]}{\sqrt{(\pi-\theta)(1+\delta_{m1})}}. \tag{6b}
$$

For convenience, we define the following four diagonal matrices:

$$
[J]_{mn} = \delta_{mn}J_{n-1}(k_cb) \tag{7a}
$$

$$
[J']_{mn} = \delta_{mn}J_{n-1}'(k_cb) \tag{7b}
$$

$$
[Y]_{mn} = \delta_{mn}[J_l(k_cb)Y_l'(k_ca) - Y_l(k_cb)J'l(k_ca)] \tag{7c}
$$

$$
[Y']_{mn} = \delta_{mn}[J_l'(k_cb)Y_l'(k_ca) - Y_l'(k_cb)J_l'(k_ca)]. \tag{7d}
$$

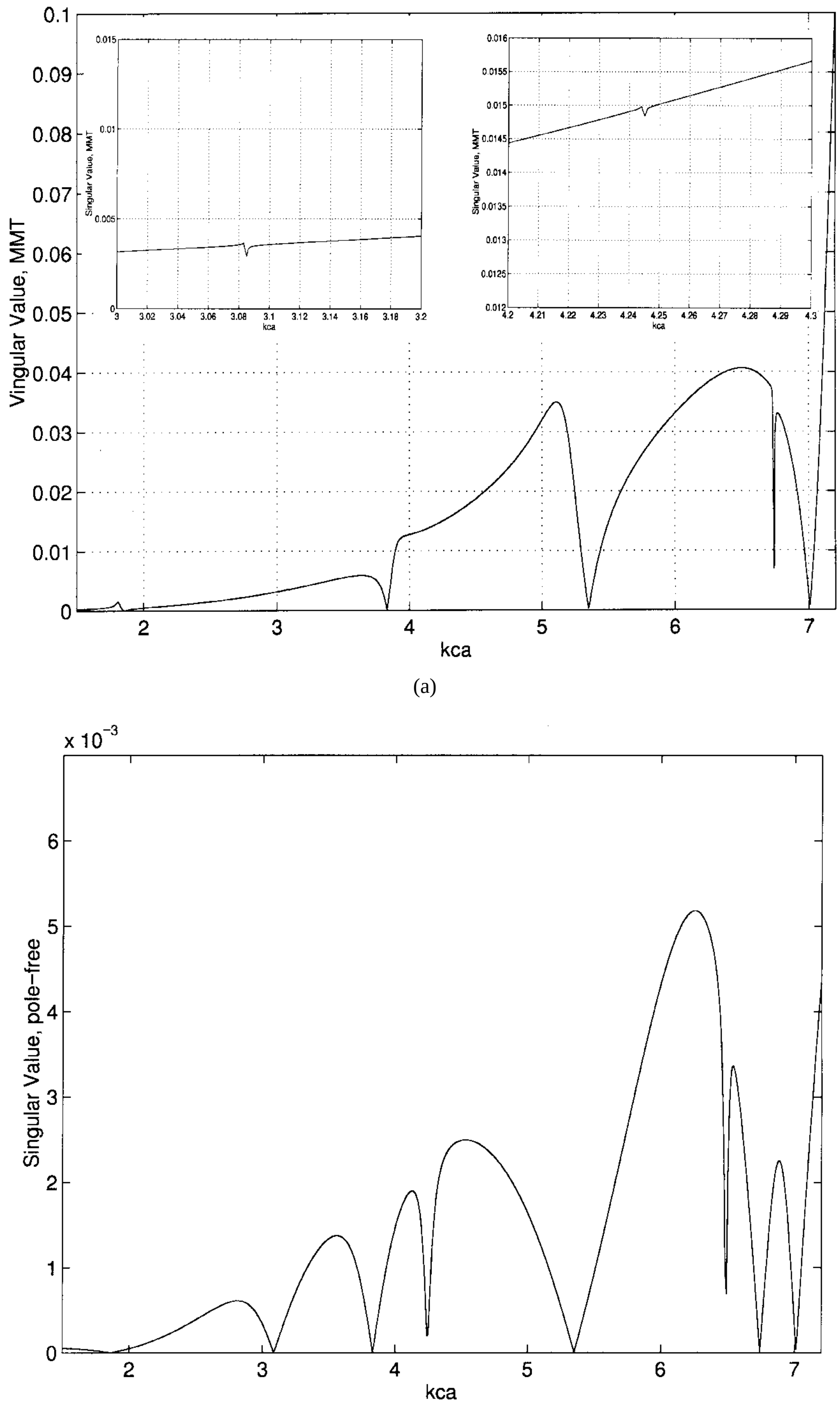

Fig. 3. Minimum singular value of $[A(k_c a)]$ as a function of $k_c a$ when $h/a = 0.9, \theta = 2.29°$, and $M = N = 6$. (a) Standard MFMT and (b) pole-free MFMT.

We also introduce the matrix $[L]$ defined by

$$[L]_{nm} = \int_{\theta}^{2\pi-\theta} d\phi \frac{\cos[(n-1)\phi]}{\sqrt{\pi(1+\delta_{n1})}} \; \frac{\cos[(m-1)\pi \dfrac{\phi-\theta}{\pi-\theta}]}{\sqrt{(\pi-\theta)(1+\delta_{m1})}}. \quad (8)$$

It is straightforward to verify that (6) can be rewritten in the following matrix form:

$$[J'][A] = [L][Y'][B] \quad (9a)$$

and

$$[Y][B] = [L]^T [J][A]. \quad (9b)$$

Note that up to this point we have carefully avoided any divisions. Equation (9) can be combined to obtain a homogeneous matrix equation in one set of the expansion coefficients $[A]$ or $[B]$. Using $[B]$ from (9b) in (9a), we get

$$[J'][A] - [L][Y'][Y]^{-1}[L]^T[J][A] = 0. \quad (10)$$

This equation is not convenient as it contains the inverse of $[Y]$ which has poles. To eliminate this pathology, we first multiply (10) from the left by $[L]^{-1}$ to obtain

$$[L]^{-1}[J'][A] - [Y'][Y]^{-1}[L]^T[J][A] = 0. \quad (11)$$

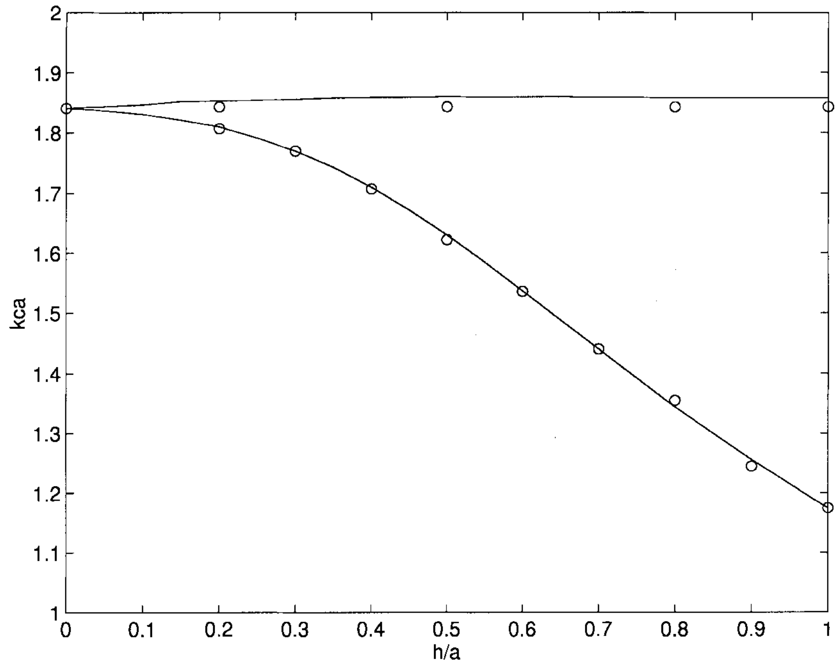

Fig. 4. Cutoff wavenumber of a ridged circular waveguide as a function of h/a when $\theta = 2.29°$. The circles are from [9].

Since the matrices $[Y']$ and $[Y]^{-1}$ are diagonal, they *commute*; their order in (11) can be reversed. We, therefore, multiply (11) from the left by $[Y]$, after the previous reversal of order, to get

$$\{[Y][L]^{-1}[J'] - [Y'][L]^T[J]\}[A] = [K][A] = 0. \qquad (12)$$

The cutoff wavenumbers of the modes under consideration are, therefore, given by the following determinantal equation:

$$\det\{[K]\} = \det\{[Y][L]^{-1}[J'] - [Y'][L]^T[J]\} = 0. \qquad (13)$$

It is now evident that (13) contains only terms which are *finite* and cannot exhibit any poles. The dashed line of Fig. 2 shows a typical plot of the determinant given by (13) as a function of $k_c a$ for the same dimensions as those of the solid line of the same figure. Note that the physical zeros of the two determinants coincide. It is also worth emphasizing the fact that the matrix multiplications appearing in (13) involve diagonal matrices and can be written explicitly as

$$[K]_{mn} = [Y]_{mm}[L]^{-1}_{mn}[J']_{nn} - [Y']_{mm}[L]_{nm}[J]_{nn}. \qquad (14)$$

In the case where unequal numbers of modes are used, the singular-value decomposition is used in both computing the inverse of the matrix $[L]$ as well as the minimum singular value of the matrix $[K]$.

As mentioned earlier, the use of the minimum singular value to locate the cutoff wavenumbers instead of the determinant circumvents the problem of the poles. The presence of the poles in the matrix is, however, reflected in the sharpness of the minima of the smallest singular value. Fig. 3(a) shows the smallest singular value obtained from the standard MFMT by carrying out the singular-value decomposition of the matrix in (5) as a function of $k_c a$ when six modes are used in each region. A step of 0.01 in $k_c a$ was used in generating this curve. Fig. 3(b) shows the smallest singular value of the matrix $[K]$ in (13) for the same number of modes and dimensions and the same step in $k_c a$. It is evident that only five minima were wide enough to be resolved with this step when the standard MFMT is used, while the new pole-free version allows the resolution of eight modes using the same step. A step of 0.001 (ten times smaller) was necessary to locate the two minima at $k_c a = 3.084$ and $k_c a = 4.245$ [see insets of Fig. 3(a)] when the standard MFMT is used. The sharper minimum at $k_c = 6.55$ was not located even with this small step width. It then becomes obvious that the pole-free formulation leads to a considerable reduction in CPU times.

In addition, the smoothness of the determinant within the new pole-free version allows the use of rapidly converging root-finding algorithms. In cases where large matrices are used, and to avoid overflows in the determinant, it may be advantageous to use only its sign in conjunction with the bisection method. The sign of the determinant can always be computed, even if the determinant itself causes an overflow or underflow, by proper scaling of the entries of the matrix.

For comparison, Fig. 4 shows results for the cutoff wavenumbers as obtained from the present technique. The circles are from [8]. The agreement of the two calculations is excellent. Furthermore, the cutoff wavenumbers of the modes with an electric-wall symmetry obtained from this paper agree with those of the sectoral and empty waveguides in the proper limits, $h/a \to 0$ and $h/a \to 1$ [9].

III. Conclusions

An efficient technique to eliminate poles from the MFMT as applied to eigenvalue problems in electromagnetics was presented. The poles are caused by inversion of singular matrices in the construction of the determinantal equation. By avoiding such inversions, a pole-free and well-behaved determinantal equation results. The minima of the smallest singular value are much wider that those obtained from the standard MFMT, thereby resulting in a substantial reduction in CPU times required to locate the zeros.

References

[1] T. Itoh, Ed., *Numerical Techniques for Microwave and Millimeter-Wave Passive Structures*. New York: Wiley, 1989.

[2] R. Sorrentino, Ed., *Numerical Methods for Passive Microwave and Millimeter-Wave Structures*. Piscataway, NJ: IEEE Press, 1989.

[3] C. A. Olley and T. E. Rozzi, "Systematic characterization of the spectrum of unilateral finlin," *IEEE Trans. Microwave Theory Tech.*, vol. MTT-34, pp. 1147–1156, Nov. 1986.

[4] A. S. Omar and K. Schunemann, "Pole-free formulation for the determination of finline modes," in *SBMO Int. Microwave Symp. Proc.*, Rio de Janeiro, Brazil, July 1987, pp. 477–481.

[5] J. Bornemann, "Comparison between different formulations of the transverse field-matching technique for the three-dimensional analysis of metal-finned waveguide resonators," *Int. J. Numer. Model.*, vol. 4, pp. 63–73, Mar. 1991.

[6] V. A. Labay and J. Bornemann, "Matrix singular-value decomposition for pole-free solutions of homogeneous matrix equations as applied to numerical modeling methods," *IEEE Microwave Guided Wave Lett.*, vol. 2, pp. 49–51, Feb. 1992.

[7] U. Balaji and R. Vahldieck, "Radial mode matching analysis of ridged circular waveguides," *IEEE Trans. Microwave Theory Tech.*, vol. 44, pp. 1183–1186, July 1996.

[8] R. Behe and P. Brachat, "Compact duplexer-polarizer with semicircular waveguide," *IEEE Trans. Antennas Propagat.*, vol. 39, pp. 1222–1224, Aug. 1991.

[9] A. Elsherbeni, D. Kaifez and S. Zeng, "Circular sectoral waveguides," *IEEE Trans. Antennas Propagat.*, vol. 33, pp. 20–27, Dec. 1991.

An Application of FDTD in Studying the End Effects of Slotline and Coplanar Waveguide with Anisotropic Substrates

Jaideva C. Goswami and Raj Mittra

***Abstract*— In this paper, the finite-difference time-domain (FDTD) method is applied in conjunction with the generalized pencil of function (GPOF) technique to evaluate the reflection coefficient from shorted slotlines and coplanar waveguides (CPW) on anisotropic substrates, and to extract the propagation constant along the line from these data. For each frequency, the field solutions at different locations are processed by using the GPOF technique to extract two complex exponents that correspond to the forward and backward traveling waves, which provide all the information about the reflection coefficient and the dispersion characteristic of the transmission line. The advantage of combining the GPOF technique with the FDTD method is that the reflection coefficients can be obtained with a single run. Recognizing that there is a dearth of results for the reflection coefficients of slotline and CPW-line discontinuities with anisotropic substrates, the present problem is also solved by using the spectral-domain method for the purpose of validation, and the two results are found to compare quite well with each other. For further validation, the FDTD and GPOF solutions are derived for isotropic substrates, and are compared with the published theoretical and experimental results.**

***Index Terms*— CPW, FDTD method, GPOF method, SDA, slotline, transmission-line discontinuities.**

I. Introduction

One of the most challenging difficulties encountered in the design of microwave and millimeter-wave integrated circuits is to accurately characterize various kinds of transmission-line discontinuities. Although the literature is replete with theoretical and experimental research related to microstrip discontinuities, the same cannot be said about other types of transmission lines, e.g., coupled-microstrip lines, slot lines, and coplanar waveguides (CPW's). The end effects of a number of transmission-line structures have been discussed in [1], [2]. Some experimental results on slot lines have been reported in [3] and [4], and CPW's and slot lines have been the subjects of investigation in [5]–[15]. A number of papers related to CPW lines are contained in the September 1993 issue of IEEE Transactions on Microwave Theory and Techniques. Muller *et al.* [8] have used the thru-line matrix (TLM) method to compute the inductance and virtual line length for a CPW short discontinuity. Dib *et al.* [10] have analyzed both open and shielded CPW discontinuities by using the space-domain integral-equation method. The mode-matching technique has been used by Rahman and Nguyen [14] to compute the S-parameters for three-layer step discontinuities. More recently, the finite-difference frequency-domain method has been employed in [15] for the analysis of CPW short circuits.

All of the above-mentioned literature has dealt with isotropic substrates—and the available results for anisotropic substrates are relatively few. In this paper, we analyze the slotline and CPW discontinuities on anisotropic substrates by using the full-wave finite-difference time-domain (FDTD) method, which enables us to obtain the characteristics of the discontinuities over a wide range of frequencies with a single run.

In the conventional approach of analyzing the discontinuities problems, an FDTD code is run twice, first for a continuous line and then in the presence of the discontinuity, to derive the time-domain fields for both the incident and reflected waves. In this paper, we combine the generalized pencil of function (GPOF) method with the FDTD method to compute the reflection coefficient in a single run. First, we obtain the field solutions over the desired frequency band at a number of equally spaced points located along the transmission line, and subsequently use the GPOF to extract two complex exponents for each frequency, which adequately represent the computed fields, and to extract the forward and backward traveling waves from these field data. The knowledge of the incident and reflected fields, in turn, yields the dispersion characteristics of the line as well as the reflection coefficient due to the discontinuity.

We use the cubic spline for the purpose of exciting the transmission line in the FDTD calculations. The time-frequency window product of the cubic spline is very close to 0.5—the lowest possible value that corresponds to Gaussian-type pulses—and the cubic spline has low-pass filter characteristics similar to the Gaussian. Consequently, for all practical purposes, the cubic spline is similar to the Gaussian and has the additional advantage of being compact in support, which in turn, avoids the need for truncation.

This paper is organized as follows. In the Section II, we discuss the FDTD solutions and their processing using the GPOF technique. To validate the FDTD/GPOF results, we also solve the present problem by using the spectral-domain analysis (SDA) which is briefly discussed in Section III. In Section IV, we discuss and compare the FDTD/GPOF and SDA results. For further validation, we apply the FDTD/GPOF to slotlines and CPW's with isotropic substrates, and compare our solutions with the published theoretical and experimental results. Finally, we present some conclusions in Section V to summarize our findings.

II. Finite-Difference Time-Domain Solution

The geometry of the problem to be studied in this paper is shown in Fig. 1. Although the figure shows the substrate with both the

Manuscript received June 11, 1996; revised April 2, 1997. This work was supported in part by the Joint Services Electronics Program under Grant N00014-96-1-0129 and in part by a Summa Foundation Fellowship.

J. C. Goswami was with the Electromagnetic Communication Laboratory, Department of Electrical and Computer Engineering, University of Illinois at Urbana-Champaign, IL 61801 USA. He is now with Schlumberger Wireline and Testing, Sugar Land, TX 77478 USA.

R. Mittra was with the Electromagnetic Communication Laboratory, Department of Electrical and Computer Engineering, University of Illinois at Urbana-Champaign, IL 61801 USA. He is now with the Department of Electrical Engineering, Pennsylvania State University, University Park, PA 16802 USA.

Publisher Item Identifier S 0018-9480(97)06074-2.